University *of Ljubljana*
Faculty *of Mathematics and Physics*

Department of Physics

Seminar I - 1st year, 2nd cycle

Rydberg atom-based radio frequency sensor

Author: Ema Stopar

Advisor: dr. Peter Jeglič

Co-advisor: Katja Gosar, mag. fiz.

Ljubljana, April 2025

Abstract

In this seminar we present Rydberg atom-based sensors that enable detection of electric fields with high sensitivity over a large frequency range. Operating at the quantum level, these receivers could surpass the sensitivity limits of classical receivers, potentially leading to a revolution in sensing and wireless communications. First, we address the main limitations of classical antennas and introduce Rydberg atoms and their convenient properties for electric field sensing. Then, we discuss the operating principles of Rydberg atom-based sensors, starting with preparation and detection of Rydberg atoms and following with radio frequency detection. We continue by presenting the experimental setup and results obtained in Laboratory for cold atoms at JSI. To conclude the seminar we present some of the research highlights in Rydberg atom radio frequency field sensing.

Contents

1 Introduction

The propagation properties of electromagnetic (EM) waves and their interaction with matter are utilized in a wide range of fields, including communications, remote sensing, healthcare technologies, and military applications. However, since Hertz's groundbreaking discovery in the 1880s, when he used a dipole antenna to demonstrate the existence of EM waves by transmitting and receiving signals, the development of transmission and reception tools has largely focused on antennas [1]. Over time, various types of antenna have been developed and optimized for different applications and operating conditions, but there have been no significant changes in the way antennas receive radio frequency (RF) signals that range from kHz to THz [2]. Traditional metal antennas have several notable limitations, creating opportunities for new technologies to address and overcome them.

1. **Low Sensitivity:** After the absorption of electromagnetic waves in an antenna the electric current is induced. Due to the thermal motion of the electrons the electric current is perturbed. This inherent noise limits the sensitivity of conventional RF detection techniques as the sensitivity of an RF receiver is defined as the minimum amplitude of the input signal that is required to produce an output signal with a specified signal-to-noise ratio, normalized to integration time [2].

2. **Limited bandwidth:** Given the antenna's optimal response to EM waves, size effects must be taken into account. In general, the antenna size l is inversely proportional to the frequency of the EM waves it transmits or receives as $l = \lambda/2$. As a result, the bandwidth of the signal that it is able to receive is constrained. For instance, a wideband dipole antenna designed for a center frequency of 10 GHz usually operates within a bandwidth that does not exceed 2.5 GHz [2, 1].

3. **Electric field distortion:** A metal detection antenna perturbs the measured electromagnetic field due to the coupling between the detected electric field and the antenna [2].

4. **Anisotropy of the radiation and detection:** Dipole antennas radiate doughnut-shaped axially symmetric fields, and similarly their detection ability depends on their direction towards the electric field.

Atom-based electric field sensors, however, operate fundamentally differently and are not limited by these constraints in the same way. Nevertheless, quantum sensors of electric field are unlikely to replace traditional receivers in mainstream applications for radio frequency signal reception, due to the convenience of the latter, but they have the potential to serve in specialized application areas where improved performance is important, such as in secure communication and high-precision sensing [3]. In this seminar, we introduce working principles of an atom-based electric field sensor operating at room temperature and show some of the experimental results that we managed to obtain in the Laboratory for cold atoms of Jožef Stefan Institute (JSI) regarding the topic. In the end, the limitations of atom-based sensors, and comparison with the classical antenna receivers will be discussed.

2 Atom-based sensors

Atom-based sensors for electric field detection typically leverage the advantageous properties of Rydberg atoms. These are atoms in states with a high principal quantum number n [4, 5]. For Rydberg atom experiments we typically use alkali metals as it is to our advantage that they have a single electron in their outermost shell, which makes the electronic structure of these atoms simpler and excitation energies to Rydberg states lower [5].

2.1 Properties of Rydberg atoms

Rydberg states have exaggerated properties compared to the ground state that make them highly promising not only for quantum sensors but also for quantum simulators and quantum computers, providing a strong motivation to study Rydberg atoms [4]. These peculiar properties of Rydberg states include the ability of coupling to radio frequency fields, a high polarizability, and very long lifetimes.

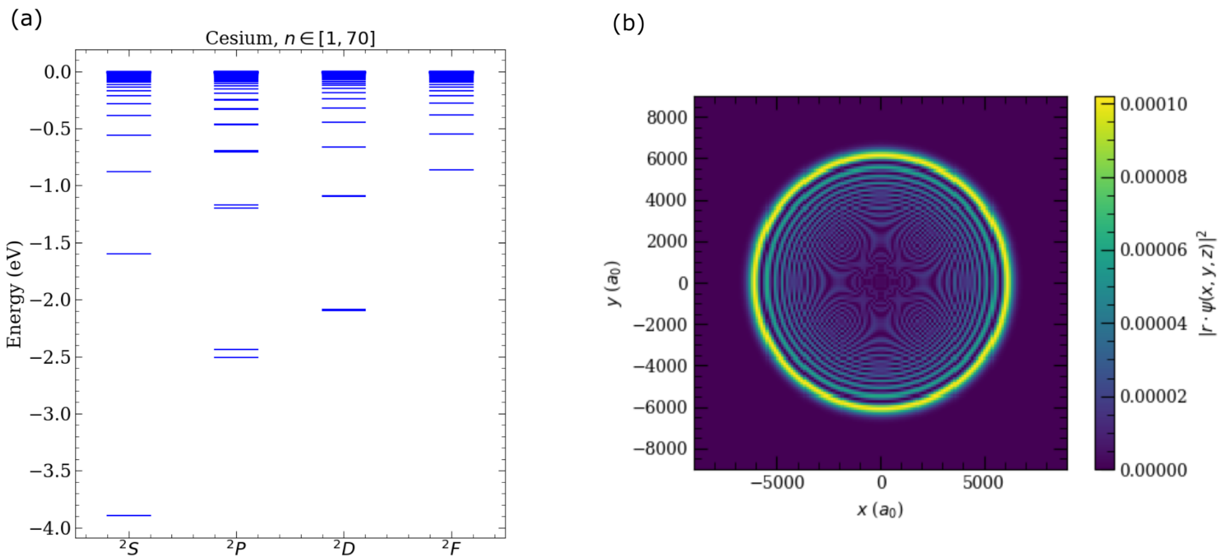

Figure 1: (a) Energy spectrum of a cesium atom; (b) Electron density projection to an xy plane of a highly excited cesium atom with $n = 60$. Adapted from Ref. 6.

1. **Coupling to radio frequency fields:** As the spacing between the energy levels of Rydberg atoms scales with n^{-3}, the energy levels for high principal numbers n are very close together [5], as shown in Fig. 1(a). Consequently, Rydberg atoms can absorb and emit radiation of frequencies in the radio frequency range, spanning from kHz to THz. This property is exploited in quantum metrology for high-precision RF field sensing that will be discussed in this seminar [1].

2. **High electric dipole moment and polarizability:**

   We can describe a Rydberg atom as an electric dipole $\mathbf{p} = -e\mathbf{d}$, where $\mathbf{d}$ is the displacement of the excited electron from the core. Since the radius of the Rydberg atoms scales with n^2 and the valence electron is very far from the core as shown in Fig. 1(b), Rydberg atoms have a very high dipole moment, which makes them highly polarizable. The polarizability of Rydberg atoms scales with n^7, making them extremely sensitive to external electric fields. This makes Rydberg atoms a promising tool for the development of highly precise electric field sensors, as well as it enables applications in quantum computing, where interactions can mediate entanglement between qubits [4].

3. **Long lifetimes:** The radiative lifetime of a Rydberg state τ_0 scales with n^3 and can be determined by summing the transition rates of all possible spontaneous emission channels as

$$\frac{1}{\tau_0} = \sum_{n'} A_{nn'}, \tag{1}$$

where $A_{nn'}$ is the Einstein coefficient for the transition from state n to a lower state n' [7, 4].

Higher n states decay more slowly, since there is very little overlap of these states with the ground state or lower excited states as lower n states are localized near the core. The lifetimes reaching hundreds of microseconds or longer make Rydberg states useful for quantum information storage and sensing applications.

Furthermore, another advantage of Rydberg atoms is that we can describe them as hydrogen-like atoms. That follows from the fact that Rydberg atoms only have one valence electron that is very far away from all the other electrons and the core. For this reason, we can simply describe a Rydberg atom as a hydrogen atom that we know analytical solutions for, with one phenomenological modification that takes into account the negative charge of the electrons in the inner shells. This approach, originally introduced by Johannes Rydberg in 1890 [8], incorporates quantum defect δ_{ln} to describe modifications that depend on the angular momentum quantum number l and the main quantum number n, determining the electron binding energy as

$$E_{nl} = -\frac{R_y}{(n - \delta_{nl})^2}, \tag{2}$$

where R_y is the Rydberg constant, $R_y = \frac{e^4 m_e}{16\pi^2 {e_0}^2 \hbar^2}$ [4]. We can introduce an effective quantum number $n_\star$ as $n_\star = n - \delta_{ln}$, replace n with $n_\star$, and use the well-known hydrogen solutions to describe a Rydberg atom [6, 2].

3 Preparation and detection of Rydberg atoms

In experimental setups, rubidium and cesium are particularly favored among alkali metals, as their transitions from the ground state to Rydberg states can be done with widely available laser technologies, meaning that transition frequencies between atomic levels match with available laser working wavelengths. For preparation of highly excited Rydberg states in the atomic vapor we excite the atoms with a weak probe laser and a strong coupling laser with respective Rabi frequencies Ω_p and Ω_c between a ground state $|g\rangle$, an intermediate excited state $|e\rangle$ and a Rydberg state $|r\rangle$ as shown in Fig. 2(a). The core technique for RF field detection using Rydberg atoms in a room-temperature atomic vapor is electromagnetically induced transparency (EIT). EIT emerges on the two-photon resonance, when Ω_p and Ω_c match the energy difference between atomic levels $|g\rangle$ and $|e\rangle$, and between $|e\rangle$ and $|r\rangle$ shown in Fig. 2(a). When the EIT condition is fulfilled, the atom evolves in the dark state $|0\rangle$,

$$|0\rangle = \frac{\Omega_c|g\rangle - \Omega_p|r\rangle}{\sqrt{\Omega_p^2 + \Omega_c^2}}, \tag{3}$$

which no longer interacts with the probe field, resulting in transparency [11, 12].

EIT is a non-destructive method that allows us to detect the states without destroying them and to read out the effect of the RF field with a photodetector. In the experimental setups for atomic RF field sensing, we typically do spectroscopy, so we measure the transmission of the probe laser light through a cesium or rubidium vapor cell as a function of the frequency of either the control beam or the microwaves (higher frequency RF field). EIT creates a narrow transmission peak of the probe laser within the broader Doppler absorption region that we get because of the Maxwell-Boltzmann distribution of atom velocities in a room temperature vapor as shown in Fig. 2(b) [13].

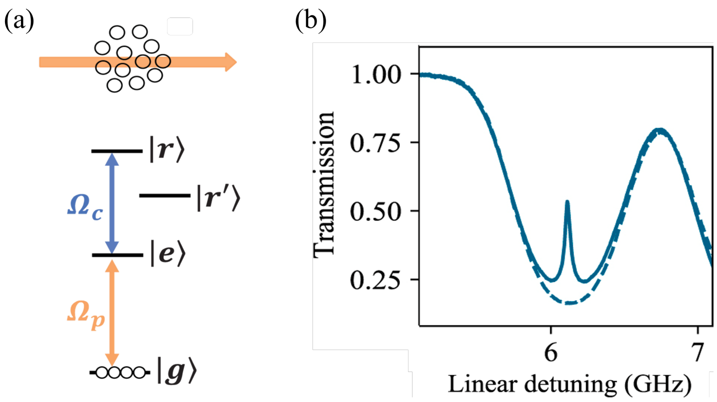

Figure 2: (a) With two laser beams we excite a two-photon transition of atoms to the Rydberg state $|r\rangle$. Due to the EIT emerging the vapor becomes transparent for the probe beam. State $|r'\rangle$ is just another Rydberg state that does not match with laser frequencies. (b) Scanning the control beam frequency on a small interval and observing the signal from the photodiode on the oscilloscope we get a Doppler broadened absorption line (dashed line) with a narrow transmission peak (solid line) caused by EIT condition being fulfilled. The figure is adapted from Ref. 9 and Ref. 10.

4 Radio frequency field detection

As we have seen before, Rydberg atoms possess a rich energy spectra that covers an ultra-wide radio frequency range. However, the measurements of RF fields are limited to discrete frequencies with narrow bandwidth that are resonant or near-resonant with transitions between Rydberg levels. To achieve continuous-frequency microwave field detection with high sensitivity we exploit the Stark effect that splits and modifies energy levels in the presence of an external electric field, analogously to the Zeeman effect in the magnetic field, as shown in Fig. 3 [14]. Fields that are not resonant with any transition to the neighboring Rydberg states induce the so called Stark shifts of the atomic levels, while resonant fields cause the Autler-Townes splitting of the EIT peak, as shown in Fig. 4. As a consequence, the EIT response is modified in predictable ways, and these effects can be used to determine the strength of the external field or to receive a signal by modulating the field [13].

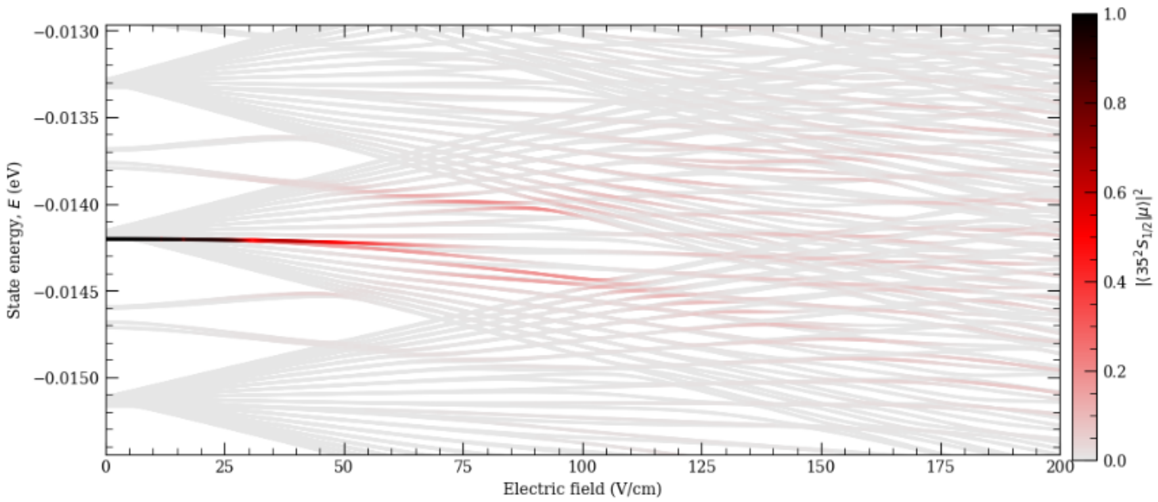

Figure 3: Stark effect on cesium levels with $n \in [30, 40]$. Energy levels experience splitting with the electric field increasing. Adapted from Ref. 6.

4.1 Stark shift

The strength of non-resonant fields such as low-frequency and DC electric fields can be determined by measuring the Stark shift Δf_S of the EIT peak. The frequency shift of the EIT peak Δf_S shown in Fig. 4(b) is quadratically dependent on the amplitude of the electric field $|E|$ by

$$\Delta f_S = \frac{\alpha}{2}|E|^2, \tag{4}$$

where α is the polarizability of the atom [2, 13].

4.2 Autler-Townes splitting

When applying the resonant RF field that couples two of the close Rydberg states $|r\rangle$ and $|r'\rangle$ the EIT peak splits as shown in Fig. 4(a). The frequency gap between the two splitting peaks is

$$\Delta f_{AT} = \frac{\mathcal{P}_{rr'}|E|}{\hbar}, \tag{5}$$

where $|E|$ is the amplitude of the applied electric field and $\mathcal{P}_{rr'}$ is the radial part of dipole matrix element of the transition between the states $|r\rangle$ and $|r'\rangle$ which can be precisely calculated. This means that by measuring the Autler-Townes splitting Δf_{AT} or the Stark shift Δf_S we can translate the measurement of the electric field strength to the measurement of the frequency, which is the most precise measurement technique ever developed [2, 13].

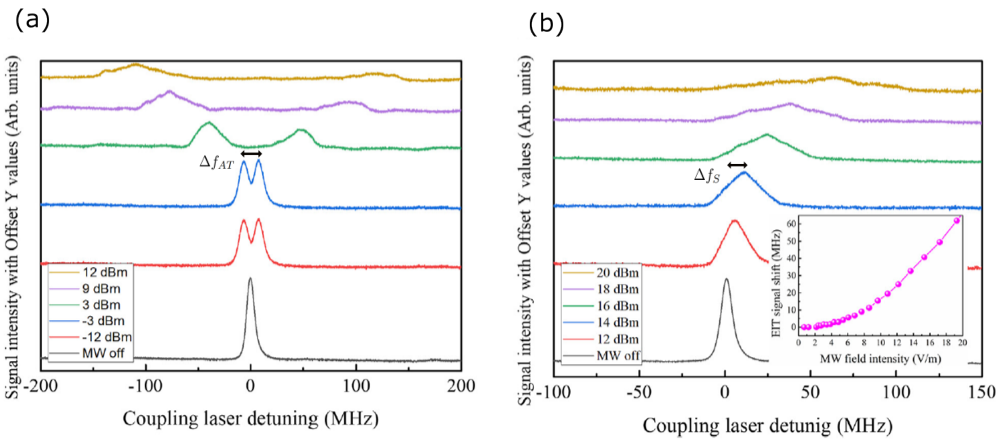

Figure 4: Effects of applying an RF field of different powers: (a) Autler-Townes splitting; (b) Stark shift. Adapted from Ref. 15.

5 Rydberg atom spectroscopy in Laboratory for cold atoms at JSI

For the spectroscopy of Rydberg states, we use a cesium vapor cell at room temperature and two laser beams. We use near-infrared light of 852 nm as a probe beam and green light of 509 nm as a coupling beam, and measure the transmission of the probe beam on a photodetector as shown in Fig. 5 (a). With the probe beam we excite the transition from the cesium ground state $|g\rangle$ $6S_{1/2}$ to the state $6P_{3/2}$ that serves as an intermediate state $|e\rangle$ and with the coupling laser to the Rydberg state $|r\rangle$ of choice. By varying the frequency of the coupling laser we can reach different Rydberg states $|r\rangle$ with n typically expanding from about 55 to 75, the quantum number l is, however, predetermined to either S or D by the selection rules. By applying the RF field we establish a transition process between different Rydberg states $|r\rangle$ and $|r'\rangle$ in cesium atoms as shown in Fig. 5 (b).

Turning on the microwave source of the selected frequency we cause either an Autler-Townes splitting or a Stark shift depending on the fact whether the RF field applied is resonant with any of the allowed

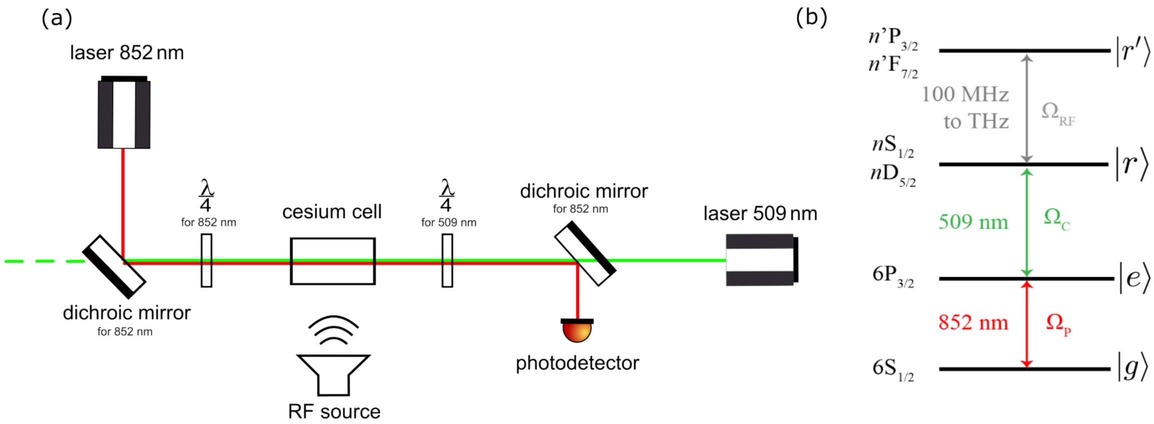

Figure 5: (a) Schematic of a simplified experimental setup in Laboratory for cold atoms at JSI. The two laser beams are overlapped and counter-propagate through the cesium vapor cell, dichroic mirrors reflect light of specific wavelengths and $\frac{\lambda}{4}$ waveplate converts between different elliptical polarizations. A photodetector is used to measure the transmission of the 852 nm light through the cesium cell, which can be exposed to microwaves of different powers and frequencies by a microwave source. (b) Excitation scheme used for detection of the RF field. Adapted from Ref. 12.

transitions to $|r'\rangle$ or not. The goal of this experiment so far was to show these different behaviours of cesium Rydberg atoms exposed to RF field experimentally. Rydberg states $|r\rangle$ are detected using the method of electromagnetically induced transparency (EIT), such that we lock the probe beam's frequency, scan the coupling beam's frequency on a small interval, and observe the transmission of the probe as a function of the coupling beam's frequency. The height of the EIT signal that corresponds to the transparency induced by excitation of the atoms to a Rydberg state depends on the presence and properties of microwaves, which can be exploited for their detection. We observed the Autler-Townes splitting of the EIT peak as a splitting and lowering of the peak, as shown in Fig. 6. In Fig. 6 we showed

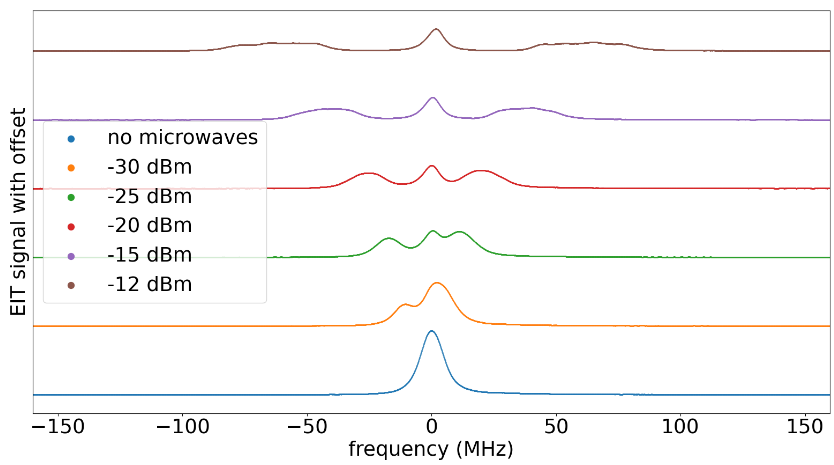

Figure 6: EIT signal corresponding to the state $60D_{5/2}$ without microwaves applied (blue) and Autler-Townes splitting of the EIT signal for increasing powers of the resonant microwave field being applied (yellow, green, red, purple, brown). A microwave field of frequency 3.21 GHz that is resonant with the transition to the $61P_{3/2}$ state and of different powers is applied.

that EIT signal changes its height and shape depending on the microwave power; it lowers and splits with microwave power increasing. Furthermore, we measured the height of the EIT peak for different microwave frequencies, shown in Fig. 7, and observed that it decreases the most when the microwave frequency matches the transition frequencies to neighboring Rydberg states. Fig. 7 shows that the peak corresponding to the EIT signal on the state $60D_{5/2}$ lowers and changes its shape at microwave frequencies that match the transition frequencies from the $60D_{5/2}$ to the $61P_{3/2}$ state. Similarly, the peak associated with the $60D_{3/2}$ state changes at microwave frequencies corresponding to the transition from the $60D_{3/2}$ state to the $61P_{1/2}$ state.

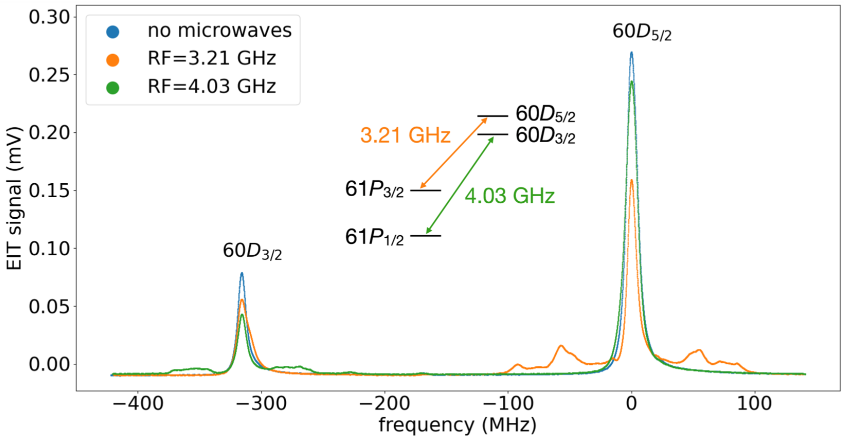

Figure 7: The transmission of the probe beam as a function of the coupling beam frequency is shown for three cases: without microwaves (blue), with microwaves at a frequency of 3.21 GHz (orange), and with microwaves at a frequency of 4.03 GHz (green).

In order to show the bandwidth dependence of our Rydberg sensor on the microwave power that is applied, we performed a different measurement. Fig. 8 shows the measurement of the change in the height of the EIT signal of the state $60D_{5/2}$, when a microwave field of different powers is applied in dependence of the microwave frequency. This is done by locking both lasers' frequencies, scanning the microwave frequency, and measuring the height change of the EIT signal. This way we can determine the bandwidth of a Rydberg sensor for different microwave powers. We observed that at low microwave powers the response is narrow and resonant around the frequency of 3.21 GHz that corresponds to the transition from the $60D_{5/2}$ to the $61P_{3/2}$, while at higher power levels the response becomes broadband. This is due to the Stark effect discussed in Section 4.

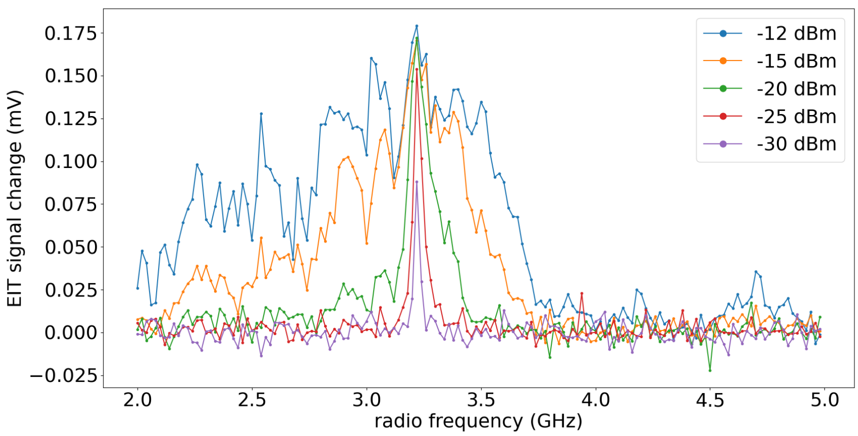

Figure 8: Measuring the height change of the EIT signal that corresponds to the state $60D_{5/2}$, when applying microwave field of different powers in dependence of microwave frequency. Microwave frequency is scanned from 2 GHz to 5 GHz and for the lowest microwave power (purple) the response is observed at the frequency of 3.21 GHz.

6 State of the art

In Section 1 we mentioned some of the main limitations of conventional antenna receivers, which are no longer a constraint for Rydberg atom receivers. First, there is no distortion of the EM field as there is no electrical circuit near the dielectric vapor cell of the atom-based sensor [16]. Second, they serve as isotropic RF field sensors, and third, since Rydberg atoms exhibit a dense spectrum of energy levels, allowing electrons to interact with various radio frequencies via the transition between different energy levels, they serve as a very broadband sensor. It has been calculated that a single Rydberg atom sensor can detect signals across an extensive frequency range, spanning from MHz to THz fields [1]. Finally, Rydberg atom receivers' sensitivity is not limited by the thermal noise as the classical antenna receivers', but by the quantum shot noise instead. It originates from the inherent randomness in quantum state measurements and it gives us the theoretical sensitivity limit of a Rydberg atom RF field sensor that equals

$$E_{\min} = \frac{\hbar}{|p|}\sqrt{\frac{1}{N_a T_r}}, \tag{6}$$

where p is the electric dipole moment, N_a is the number of participating atoms, and T_r the coherence time of the EIT process [16].

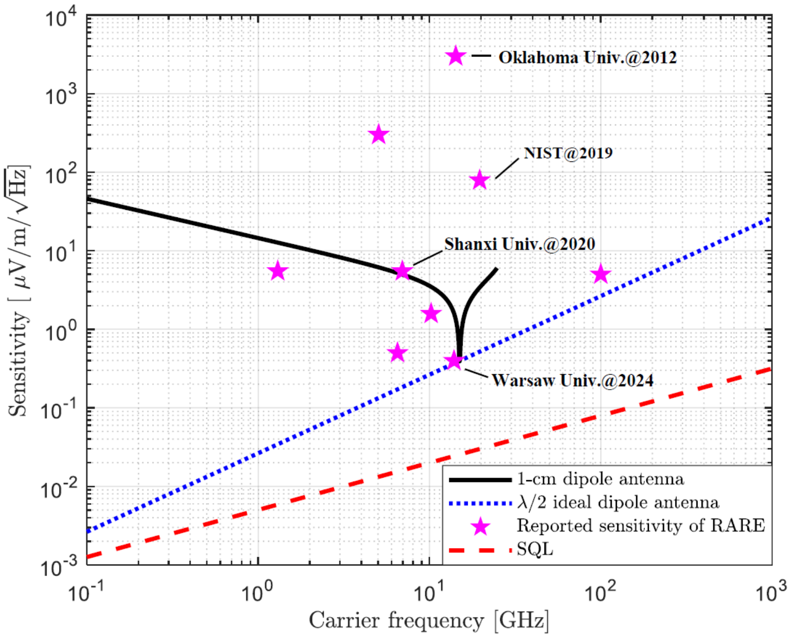

Figure 9: Sensitivity comparison between Rydberg atom receivers through the years (purple stars), a classical 1 cm long antenna (black solid line), and a classical antenna of ideal size that matches the desired frequency we want to detect (dashed blue line). A standard quantum limit is plotted with red dashed line. Adapted from Ref. 1.

Fig. 9 compares the sensitivity of a Rydberg atom receiver with conventional antennas. Representative values of $T_r = 225\,\mu s$ and $N_a = 5 \times 10^5$ from Ref. 16 are used. The dipole moment p is selected based on the electron transition $nD_{5/2} \leftrightarrow (n+1)P_{3/2}$.

To establish a meaningful comparison, we also consider the sensitivity limit of a 1-cm dipole antenna, as its physical dimensions are comparable to those of a typical vapor cell used in Rydberg atom receivers. Fig. 9 demonstrates that the standard quantum limit can exceed the sensitivity of conventional $\lambda/2$ dipole antennas by several orders of magnitude.

Since the initial experimental realization of Rydberg atom receivers in 2012 at Oklahoma University [17], the sensitivity has improved by a factor of 10^4. Recently, the state of the art Rydberg sensors have not only outperformed similarly sized dipole antennas but also achieved sensitivities comparable to dipole antennas of ideal length for a frequency measured, when $l = \lambda/2$. In 2024 a new benchmark was set by

Warsaw University [18], managing to eliminate background noise better and achieving a sensitivity as low as $0.4\,\mu\text{V/m}/\sqrt{\text{Hz}}$ at 13.9 GHz.

Looking ahead, it is anticipated that Rydberg receivers will surpass the fundamental sensitivity limits of ideal antennas and approach the standard quantum limit [1].

7 Conclusions

The main limitations of the classical antenna receivers are low sensitivity, limited bandwidth, directional dependence and inevitable distortion of the electric field measured. However, they all can be successfully addressed by Rydberg-atom receivers. Rydberg atoms exhibit exaggerated properties that are advantageous in radio frequency field sensing. These are very long lifetimes, extremely high polarizability and the ability of coupling to RF fields. We build a Rydberg atom-based sensor by exciting some cesium or rubidium vapor in the cell using two laser beams; a probe and a coupling laser beam, and we measure the transmission of the probe beam through the cell. For detection of the Rydberg states, we use electromagnetically induced transparency, which does not destroy Rydberg states and creates a narrow transmission peak that we detect on a photodiode. When we add a radio frequency field, the EIT signal experiences the Stark effect, that can be used to determine the strength of the external field or to receive a signal by modulating the field. The described technology enables the development of highly sensitive, broadband microwave sensors for secure communication and high-precision electric field sensing. We present the experimental setup and results obtained in Laboratory for cold atoms at Jožef Stefan Institute. Lastly, we make a comparison between the classical electric field receivers and Rydberg atom-based sensors and conclude that Rydberg receivers will surpass the fundamental sensitivity limits of ideal antennas and approach the standard quantum limit that can exceed the sensitivity of conventional antennas by several orders of magnitude.

Bibliography

[1] M. Cui, Q. Zeng, and K. Huang, *Rydberg atomic receiver: Next frontier of wireless communications*, (2024), arXiv:2412.12485 [eess.SP] .

[2] H. Zhang, Y. Mac, K. Liao, W. Yang, Z. Liu, D. Ding, H. Yan, W. Li, and L. Zhang, *Rydberg atom electric field sensing for metrology, communication and hybrid quantum systems*, Elsevier **69**, 1515–1535 (2024).

[3] C. T. Fancher, D. R. Scherer, M. C. S. John, and B. L. S. Marlow, *Rydberg atom electric field sensors for communications and sensing*, IEEE Transactions on Quantum Engineering **2**, 1–13 (2021).

[4] T. F. Gallagher, *Rydberg atoms*, Reports on Progress in Physics **51**, 143 (1988).

[5] Wikipedia: Rydberg atoms, accessed: March, 2025.

[6] K. J. W. C. S. A. N. Šibalić, J. D. Pritchard, Arc: An open-source library for calculating properties of alkali rydberg atoms (2017), accessed: March, 2025.

[7] X. Wu, X. Liang, Y. Tian, F. Yang, C. Chen, Y.-C. Liu, M. K. Tey, and L. You, *A concise review of Rydberg atom based quantum computation and quantum simulation*, Chinese Physics B **30**, 020305 (2021).

[8] J. Rydberg, *On the structure of the line-spectra of the chemical elements*, Philosophical Magazine **29**, 331–337 (1890).

[9] W. Xu, A. V. Venkatramani, S. H. Cantú, T. Šumarac, V. Klüsener, M. D. Lukin, and V. Vuletić, *Fast preparation and detection of a Rydberg qubit using atomic ensembles*, Phys. Rev. Lett. **127**, 050501 (2021).

[10] C. R. Higgins and I. G. Hughes, *Electromagnetically induced transparency in a v-system with 87rb vapour in the hyperfine paschen-back regime*, Journal of Physics B: Atomic, Molecular and Optical Physics **54**, 165403 (2021).

[11] J. D. Pritchard, A. Gauguet, K. J. Weatherill, and C. S. Adams, *Optical non-linearity in a dynamical Rydberg gas*, Journal of Physics B: Atomic, Molecular and Optical Physics **44**, 184019 (2011).

[12] R. Finkelstein, S. Bali, O. Firstenberg, and I. Novikova, *A practical guide to electromagnetically induced transparency in atomic vapor*, New Journal of Physics **25**, 035001 (2023).

[13] M. T. Simons, A. B. Artusio-Glimpse, A. K. Robinson, N. Prajapati, and C. L. Holloway, *Rydberg atom-based sensors for radio-frequency electric field metrology, sensing, and communications*, Measurement: Sensors **18**, 100273 (2021).

[14] D. Song, Y. Jiao, J. Hu, Y. Yin, Z. Li, Y. He, J. Bai, J. Zhao, and S. Jia, *Continuous broadband Rydberg receiver using AC Stark shifts and Floquet states*, Applied Physics Letters **125**, 194001 (2024).

[15] Y. Du, N. Cong, Y. Liu, Z. Lyu, J. He, and R. Yang, *Enhanced microwave-atom coupling via quadrupole transition-dressed Rydberg atoms*, Frontiers in Physics **12**, 10.3389/fphy.2024.1312930 (2024).

[16] H. Fan, S. Kumar, J. Sedlacek, H. Kübler, S. Karimkashi, and J. P. Shaffer, *Atom based RF electric field sensing*, Journal of Physics B: Atomic, Molecular and Optical Physics **48**, 202001 (2015).

[17] S.-A. K. H. e. a. Sedlacek, J., *Microwave electrometry with Rydberg atoms in a vapour cell using bright atomic resonances*, Nature Physics **8**, 819–824 (2012).

[18] P.-U. M. M. e. a. Borówka, S., *Continuous wideband microwave-to-optical converter based on room-temperature Rydberg atoms*, Nature Photonics **8**, 32–38 (2024).